Design and analysis of supersonic business jet concepts

Sriram. K. Rallabhandi* and Dimitri N. Mavris†
Georgia Institute of Technology, Atlanta, GA 30332

Supersonic business jet design is a complex process to balance highly stringent environmental requirements in addition to the usual performance measures. Conceptual aircraft designs obtained by employing simplified analyses would be compromised in some respect when the concept is transferred to further stages of design. To overcome this problem, improved analysis methods for conceptual aircraft design are developed in this study. Geometry is parameterized using many shape parameters to create any arbitrarily complex aircraft shape. The aerodynamic flow field near the aircraft is obtained in an automated fashion using three dimensional panel methods. Sonic boom propagation is carried out considering atmospheric variations, thermo-viscous absorption, molecular relaxation and diffusion phenomena. The optimization results obtained elsewhere using simple linear methods are analyzed using the methods developed here and the responses are compared. Shortcomings of the traditional approaches are discussed and future work using these improved methods is suggested.

Nomenclature

c	Ambient speed of sound.
FFT	Fast Fourier Transform.
h	Percentage of atmospheric molecules having water.
P_{ref}	Standard atmospheric pressure.
RH	Relative humidity in %.
T_{ref}	Reference atmospheric temperature.
T_t	273.16 K, Triple point isothermal temperature.
Δk_I	Dispersive Imaginary wave number.
Δk_R	Dispersive real wave number.
κ	Coefficient of thermal conductivity.
μ	Coefficient of viscosity.
μ_B	Coefficient of bulk viscosity.
ν	Number of relaxation mechanisms.
ω	Characteristic frequency.
τ_ν	Relaxation parameter for the ν type molecule.

*Postdoctoral Fellow, Aerospace Systems Design Lab, AIAA member.
†Director and Boeing Professor of Advanced Aerospace Systems Analysis, Aerospace Systems Design Lab, Associate Fellow AIAA

I. Introduction and Motivation

THERE has been a recent surge of interest in the design of supersonic business jets [1,2], given the market demand and time savings they offer. However, to make these designs commercially and economically viable, many technical challenges have to be overcome. Sonic booms have been the technical showstoppers to allow supersonic flight over populated regions. When sonic boom minimization is added to the optimization of other traditional performance measures, the viable design space is extremely small. It is necessary to perform a multi-disciplinary analysis by simultaneously considering numerous responses of interest to study the relevant trade-offs.

Traditional aircraft design process involves three distinct design phases: conceptual, preliminary and detailed design. With the ever increasing computational power, the distinction between conceptual and preliminary design phases is progressively getting blurred. Modern aircraft design requirements impose a significant pressure to conduct advanced multi-disciplinary analyses and design from the conceptual phases because at this stage the design freedom and flexibility are at their maximum [3]. In order to reap the maximum benefit, the designer has to take advantage of the huge design space up-front to avoid serious and costly alterations in design during the later stages. To analyze the large conceptual space, better analyses methods must be used but at the same time consideration has to be given to minimize the computational time to perform such analyses. It is the belief of the authors that this balance of accuracy and time can be achieved by resorting to improved geometry models and better aerodynamic and aero-acoustic methods in the early phases of design. The following sections briefly describe the constituents of a multi-disciplinary conceptual environment envisioned for selecting supersonic aircraft concepts.

II. Geometry generation and discretization

Previous conceptual studies [4,5] on supersonic business jet design have led the authors to conclude that in order to realize practical designs, better analysis methods have to be employed. The analyses should capture the effect of geometry to a greater extent than has been achieved in the past using conceptual techniques. It is generally realized that conceptual analyses differ greatly from high fidelity methods. Not only do they produce low fidelity results, but also represent the geometry of the aircraft in an inadequate fashion so that they cannot be readily used to run high fidelity analysis. When supersonic aircraft are designed to overcome extremely difficult objectives such as simultaneous optimization of sonic boom and cruise efficiency, linear methods may be ill-suited for certain geometries which do not meet the slender body assumption or other cases where non-linear effects may be dominant. In these situations, it would be extremely helpful to utilize higher order methods to yield satisfactory results. However, running higher fidelity analysis requires geometry representation in a meshed, watertight format. It is difficult to represent the geometry in an accurate and consistent format for all levels of analyses. For complex geometries, mesh generation and other pre-processing steps may consume more time than the actual CFD flow solution computation. Generating various geometries that are suitable for a wide range of aerodynamic analyses is extremely difficult and problematic. However, if this challenge is not overcome, conceptual analysis methods may produce questionable results for certain geometries, which cannot be easily verified using high fidelity methods. For this reason and perhaps many more, a technique by which many geometries can be automatically generated and discretized in a quick and efficient manner is required during conceptual design.

A geometry generation and discretization method proposed by the authors [6] is a suitable fit for this requirement. The idea is to use design variables to control the shape as well as the configuration of each component of the aircraft. Configuration variables signify the presence or absence of components, the number of components and other discrete choices. Furthermore, there are various continuous parameters to define the shape of each component. Shape here refers to the curvature, twist, dihedral and other local features of the aircraft components. Various engineering parameters, control points for NURBS and Bezier curves are design variables used to change the shape. The main advantage of this approach is that parametric decomposition is achieved and individual components can be modified without affecting other components.

Surface intersection operations are performed on the individual components to obtain a single watertight entity from a collection of components. The desired geometry generation framework required to allow the use of aerodynamic analyses of varying fidelity is depicted in Figure 1. The shape of each component is independent of the shape and location of other components. Component discretization and agglomeration is done using efficient geometry algorithms [7]. This geometry representation can be used as the geometry format

to carry out aerodynamic analyses ranging from linear methods to unstructured panel or CFD techniques. During the surface discretization stage, the neighboring triangle information is stored. This information along with the surface grid allows a CFD pre-processor to quickly generate the volume mesh necessary for computing the flow field. This CFD near-field signature can then be used in sonic boom prediction [8, 9] to obtain fully converged estimates of the ground signature in an efficient manner. If unstructured high fidelity methods are not available, a further surface transformation should create a structured watertight mesh that can be used in structured computational methods.

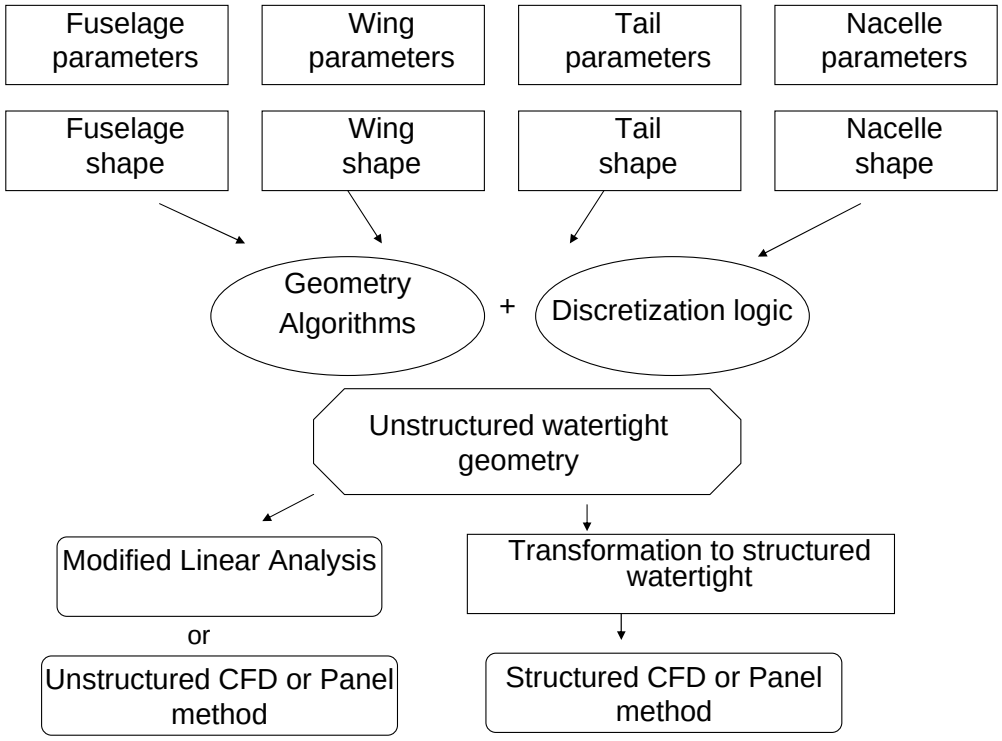

Figure 1. Geometry generation setup for aerodynamic analysis of varying fidelity

III. Near field prediction for sonic boom analysis

Traditional conceptual tools for sonic boom prediction [10, 11] are limited in their analysis capability and are widely known to be unsuitable to capture the non-linear effects of aircraft designed for sonic boom minimization because of their inherent assumptions. With these known limitations, new conceptual methods are developed to evaluate the effect of the geometry for sonic boom prediction. Changes to the geometry representation, as described in the previous section, necessitate modifications to the existing linearized methods. A design architecture was proposed by the authors [12] that not only supports linearized methods, but also has the flexibility to allow unstructured CFD or potential flow analysis methods to be attempted efficiently. Accurate equivalent area due to volume of any arbitrary body can be computed [13] by directly operating on the unstructured watertight geometry. However, traditional linear methods are limited in their applicability and CFD is too expensive. Therefore, we seek to add three dimensional panel method analyses to the automated design architecture for evaluating certain geometries that yield poor results using modified linear methods.

Three dimensional panel methods offer a perfect platform to obtain the near field flow solution by providing much more accurate results when compared to the traditional linear methods while consuming far less computational time compared to CFD analysis. Studies have been conducted to use advanced [14] and multi-fidelity [15] algorithms in the design of supersonic business jets. However, these efforts are tailored towards aircraft preliminary design where computationally expensive analyses are used to study perturbations of an optimized baseline obtained using conceptual methods. This study is aimed at facilitating the use of

automated panel methods in the down-selection process of suitable supersonic configurations from the vast number of possible designs. We attempt to automate the process of panel analysis over conceptual geometries to obtain the near-field signature required for predicting the sonic boom signature on the ground.

The panel method used in the present study is called PANAIR [16, 17], a higher order structured panel method developed originally at Boeing. The fundamental challenge to run PANAIR over conceptual geometries is its requirement that the geometry be represented by contiguous panels without any gaps. This is a considerable challenge when different components are loosely connected to form a vehicle configuration. Using the unstructured watertight representation generated using the geometry algorithms, an unstructured panel method can be used without further surface mesh processing. However, since such a tool was not available, surface mesh operations that transform an unstructured surface mesh into a structured representation are developed. This transformation process is broken down into three sub-problems. The first aspect is to obtain the three dimensional curves of intersection between the various intersecting components. The second step involves splitting the geometry automatically into adjoining meshes or networks. The final step involves creating the trailing wake networks, running the panel analysis, extracting results and visualization. These are described in a little more detail in the following paragraphs.

A. Curves of intersection

Given the geometry composed of various components, component intersection information is needed to generate a well abutted structured paneling of the geometry. To obtain this information, the GNU Triangulated Surface library (GTS) [7] is used. GTS library consists of data structures for efficient manipulation of surfaces including union and intersection based on constrained Delaunay triangulation algorithm [18]. The geometry obtained using a combination of discrete and continuous variables is read into GTS data structures. Each component is triangulated, "sealed" and placed on a stack. Depending on the location of components on the stack, they are taken in turn and combined together two at a time using geometry boolean operations. If a certain combination does not intersect a component in the stack, the next component is tried. This procedure is continued until all the components in the stack are used up. Using the resulting watertight unstructured representation, the list of edges at the interface of adjoining components is obtained and processed to generate smooth three dimensional curves between any two components. Figure 2 shows the initial wire frame representation of a sample wing-body geometry along with the three dimensional curve of intersection.

B. Network splitting and abutment

Various components and their curves of intersection are used to identify the locations of components with respect to one another. The wing-body intersection is split into adjoining networks according to the logic shown in Sketch 3(a). Following this logic, the fuselage is divided into a nose region, four regions above and below the curve of intersection, and two aft portions. The aft is divided into two portions to decide the location of the wake networks. Special consideration is also made to handle situations when the intersecting curve is not closed i.e. when the wing is partially intersected by the fuselage as in the case of a high or low wing configuration. Figure 4 shows the abutted grid obtained automatically from a given wire-frame geometry. The same logic of network abutment is extended if there are more intersection regions, for example horizontal tail (3(b)) or vertical tail. Unlike some panel analysis methods, PANAIR requires the user to include wake panel information in order to predict correct flow solution. In this study, straight wakes attached to the wings and wing-body intersections while trailing wakes from the body base section are also automatically created.

C. PANAIR solution and validation

Traditional tools [19, 11, 10] do not appropriately consider the lifting effects of tail surfaces which could lead to erroneous results in the prediction of sonic boom. Using panel methods, the flow fields and sonic boom signatures with and without tail geometries can be easily compared. Capturing the tail effects on sonic boom is extremely important as they have a huge effect on the effective length of the geometry and the rear shock strength. Figures 5(a) and 5(b) depict the PANAIR flow solution as surface pressure coefficient contours over the abutted surface grid of Figure 4, with and without a T-tail respectively, at a Mach number of 2.0. The lift and drag coefficients for the no tail configuration are 152.107 and 13.164 respectively with a reference area of 1. This produces a lift to drag ratio of 11.55 without including the contribution of the friction drag.

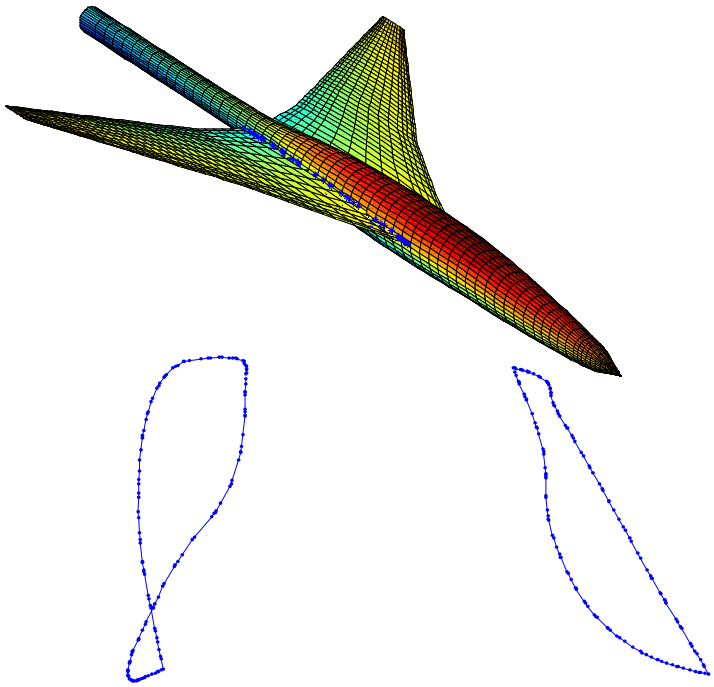

Figure 2. Curves of intersection between components

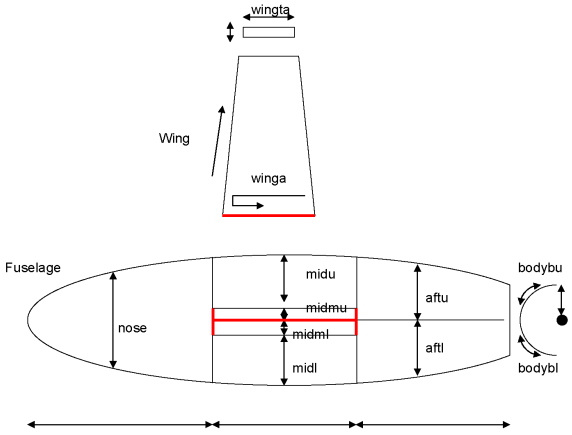

(a) **Wing and fuselage**

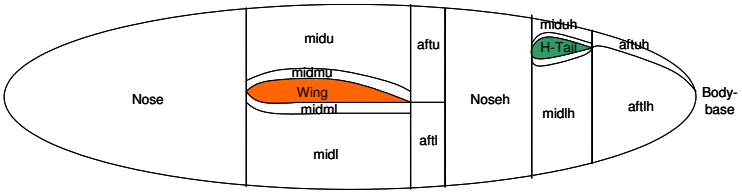

(b) **Wing, fuselage and tail**

Figure 3. Network abutment logic

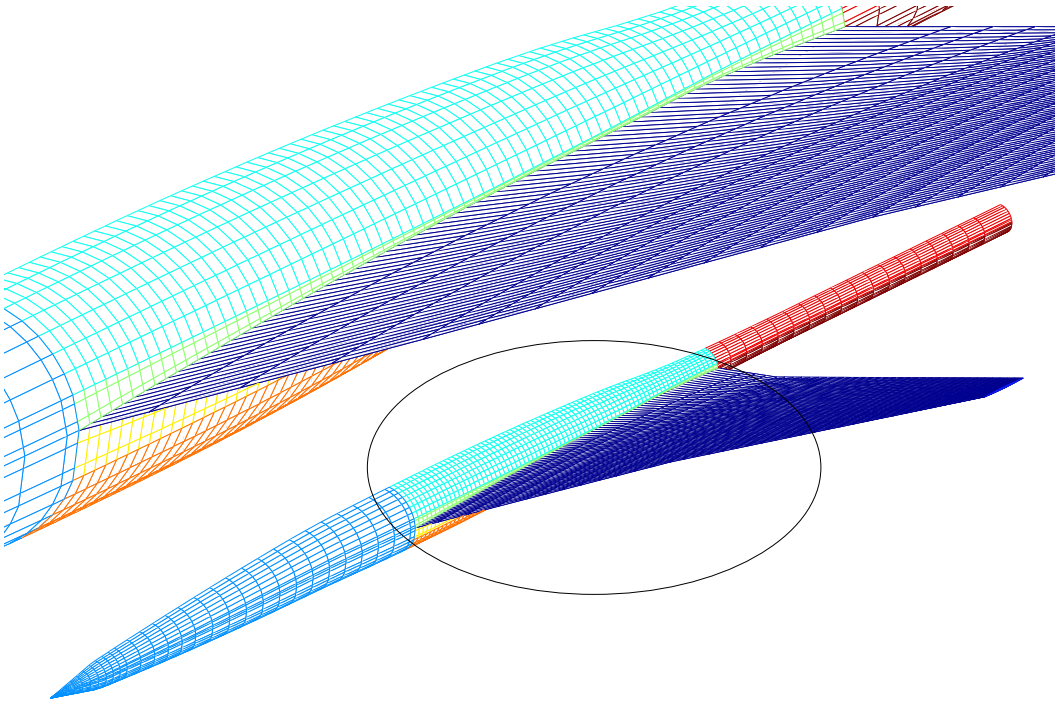

Figure 4. Automatic abutted network generation

For the configuration with the T-tail, the lift to drag ratio without including friction component is 11.35. Friction drag and zero-lift wave drag can be computed using the geometry-based analysis methods developed and reported elsewhere [6].

In order to rely on PANAIR solution results, couple of validation runs were carried out and the results are compared with published experimental data. Figure 6 compares the computed surface pressure coefficient with experimental values over the wing of a sample wing-body configuration [20] at a free stream Mach number of 1.2. It is seen that the except near the trailing edge and wing tip regions, the PANAIR prediction matches the experimental data quite well. Figure 7 compares the PANAIR results with experimental data at three fuselage locations, A, B, C as depicted in the figure. The surface pressure correlation between PANAIR and experimental measurements is quite good and the minor discrepancies towards the rear of the fuselage can be attributed to the thick boundary layer and flow separation not captured by panel methods. Although another validation test [21] was also conducted and the results match the experimental results quite well, they are not included here for the sake of brevity. From these, it is evident that the automatic surface generation, discretization and paneling is working as desired.

Once the panel analysis solution is obtained, off-body pressure signature is obtained using the location of panels and singularity strengths obtained by imposing surface flow boundary conditions. The off-body signature is used as the near-field estimate for signature propagation to the ground. Figure 8 compares the pressure signature with and without the tail for the configuration (See Figure 2) at a distance of one body length below the aircraft centerline. The front and rear shocks are very pronounced and the wing shocks and other expansions can also be observed from this signature. For the configuration with T-tail, additional shocks and expansion regions are observed towards the rear portion. A T-tail configuration not only provides a medium to trim the aircraft but also increases the effective length of the aircraft, which is a useful feature for sonic boom reduction as it separates the distance between front and rear shocks and prevents shock coalescing during atmospheric propagation. In this particular example, it is seen from the figure that for the T-tail geometry the pressure reaches ambient conditions at about 440 ft while for the configuration without tail, the same condition is reached at approximately 410 ft. Thus, T-tail adds about 30 ft to the effective length of the body.

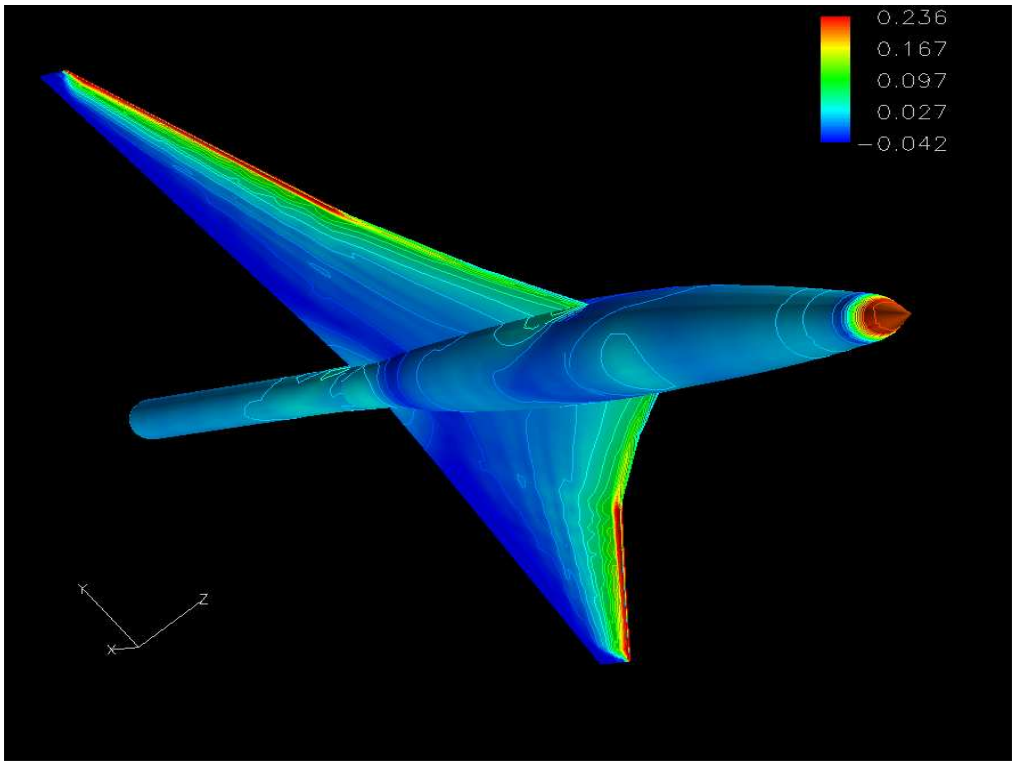

(a) **Without tail**

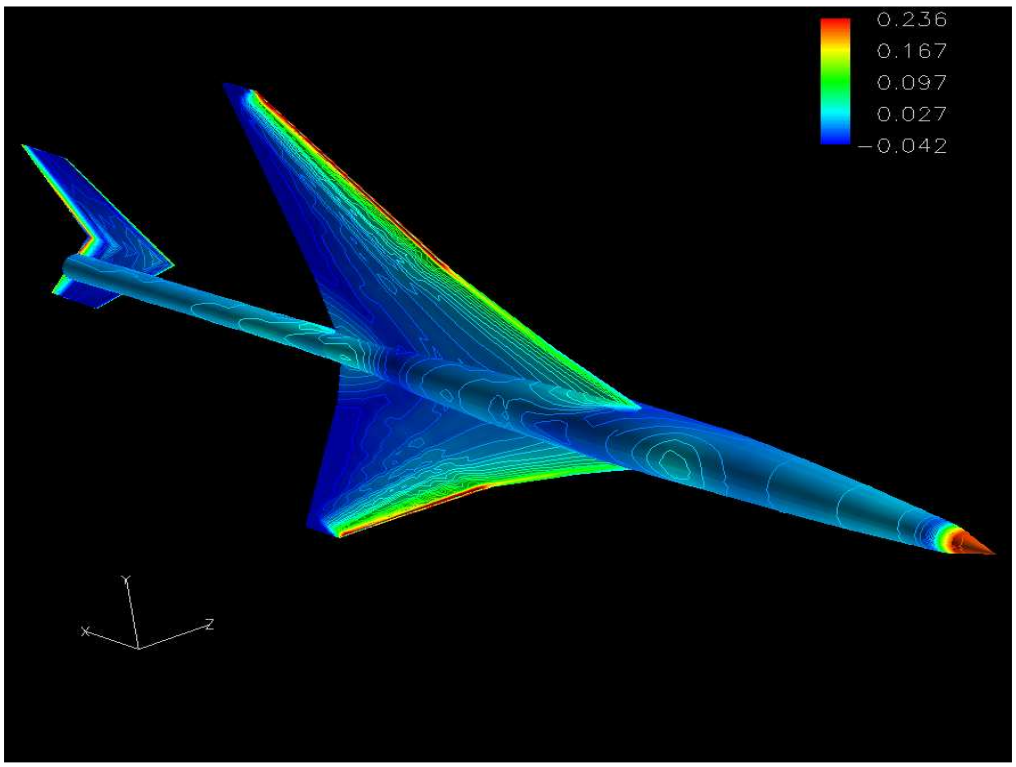

(b) **With T-tail**

Figure 5. PANAIR solution visualization

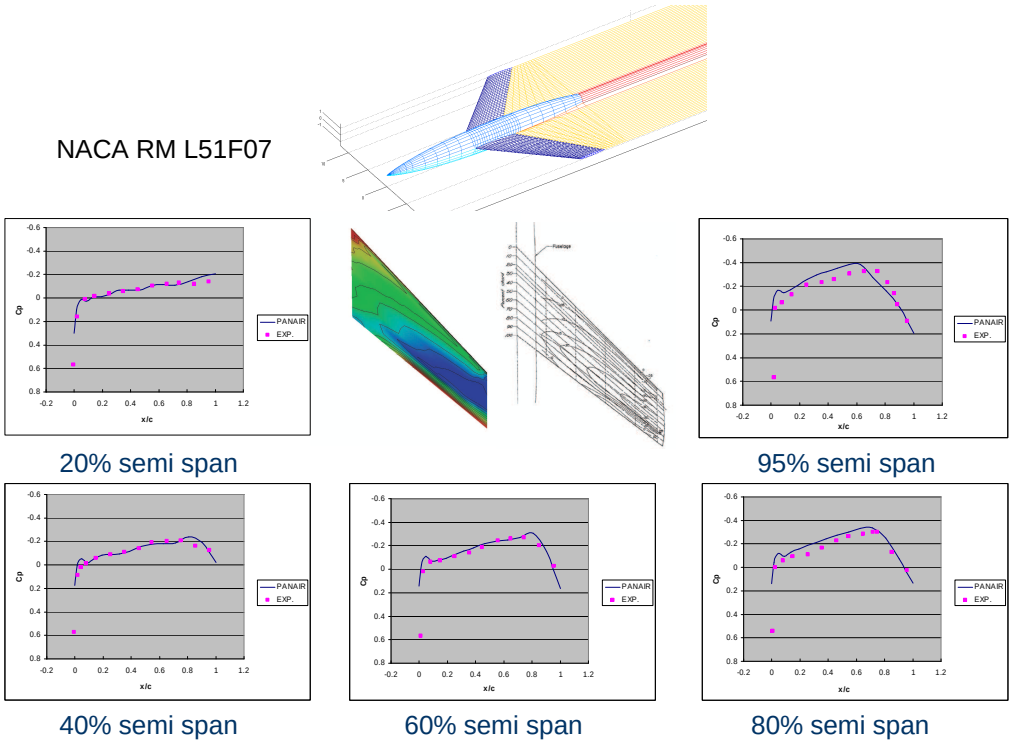

Figure 6. PANAIR solution validation over wing

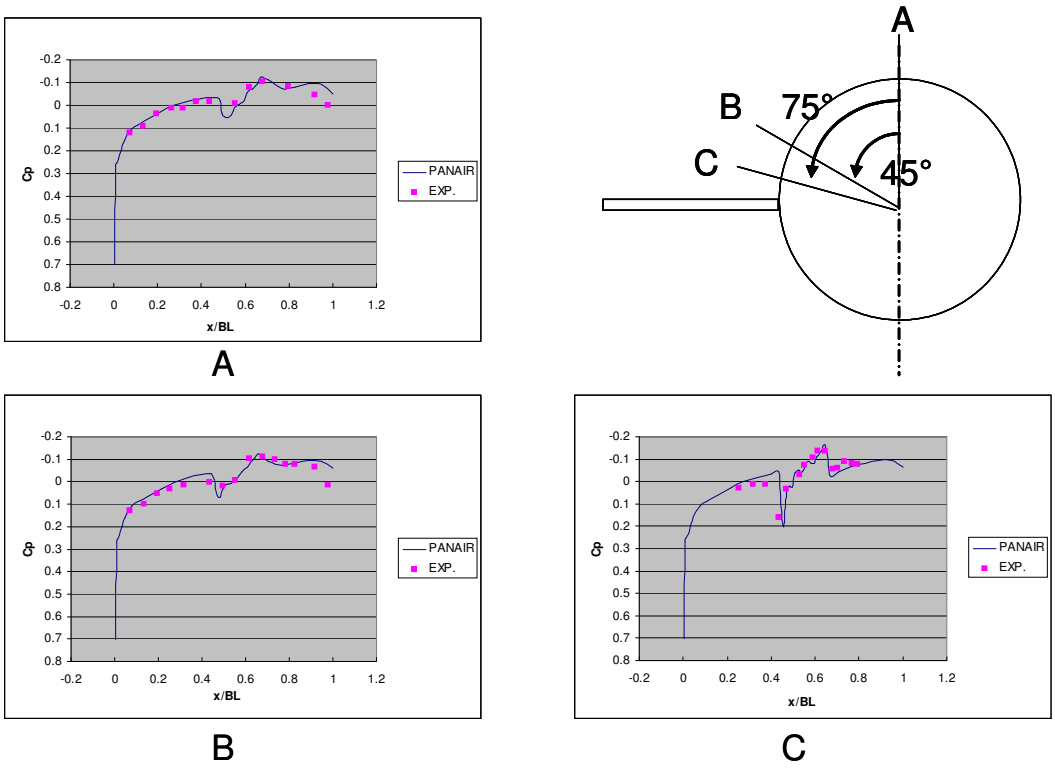

Figure 7. PANAIR solution validation over fuselage

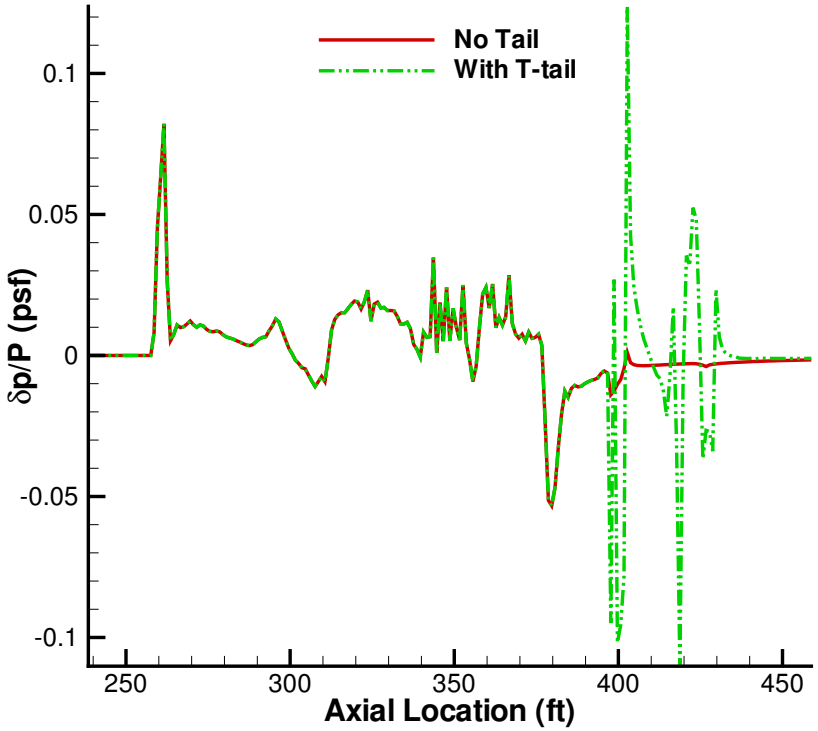

Figure 8. PANAIR offbody pressure signature comparison

IV. Non-linear propagation

Noise propagation through the atmosphere forms an important ingredient in the estimation of the sonic boom loudness on the ground. Unlike the near field pressure signature, which is determined by calculating the flow-field around the body, the ground signature is not completely under the control of the designer. This is because the noise amplitude and direction are highly dependent on the prevalent atmospheric conditions. Sonic boom variability due to atmospheric perturbations from the standard atmosphere is a topic of research [22, 6] in itself and is not of interest in this study. Effects like atmospheric absorption, molecular relaxation [23], turbulence [24] and anomalies in temperature and wind profiles influence the ground pressure signature. Most conceptual sonic boom prediction tools [11, 25] include just the non-linear steepening correction along with linearized acoustical propagation. This is known to generally over-predict the sonic boom parameters as the atmospheric attenuation is not considered. Improvements to the propagation algorithm, though not necessary in conceptual design, should be used if the computational penalty is not significant.

In this study, non-linear steepening, atmospheric absorption, diffusion and molecular relaxation effects are modeled into the propagation algorithm. These effects are modeled in the frequency domain whereas the non-linear steepening is carried in the time domain. Even though these phenomena occur simultaneously as the pressure wave propagates towards the ground, for the purpose of simplicity these phenomena are applied one after the other. This sort of approximation has been used in previous research [26] and is generally assumed to be valid. Transfer between the frequency and time domain is achieved by using the FFT and inverse FFT operations. For weak shocks, as in sonic booms, the frequency modification can be applied once in several steps without losing much in accuracy. This keeps the costly FFT operations to a minimum. The basic sonic boom propagation code that has been used is the PCBOOM [25], developed by Wyle Research Laboratories. The frequency domain corrections for absorption, diffusion and molecular relaxation are included within the functionality of PCBOOM.

A. Theoretical aspects of atmospheric absorption

In this section, the equations [27] for non-linear propagation with dissipation and relaxation are presented. It has been shown that most of the effects of pressure propagation through the atmosphere can be modeled by using the augmented Burger's equation as shown in Equation 1 and 2. The first two terms of Equation 1 represent linear propagation of waves. The third term is the correction from non-linear steepening, fourth term accounts for thermo-viscous dissipation and the last term represents molecular relaxation phenomena.

$$\frac{\partial p}{\partial t} + c\frac{\partial p}{\partial x} + \frac{\beta p}{\rho c}\frac{\partial p}{\partial x} - \delta\frac{\partial^2 p}{\partial x^2} + \Sigma_\nu(\Delta c)_\nu\frac{\partial p_\nu}{\partial x} = 0 \tag{1}$$

$$p_\nu + \tau_\nu\frac{\partial p_\nu}{\partial t} = \tau_\nu\frac{\partial p}{\partial t} \tag{2}$$

τ_ν represents the relaxation times of the atmospheric constituents. In this study, we assume that atmosphere is composed of Oxygen and Nitrogen and hence calculate only two relaxation mechanisms i.e. $\nu = 2$. The relaxation times for Oxygen and Nitrogen are calculated from Equations 3 and 4 respectively. The quantity h represents the percentage of all atmospheric molecules which have water content. RH is the relative humidity level in percentage. Viscosity μ and thermal conductivity κ are obtained using Sutherland's law. μ_B is the bulk viscosity, which has been taken to be 0.6μ. T_t is the triple point isothermal temperature, $\mathrm{P}_{ref} = 1.01325 \times 10^5$ Pa is the standard atmospheric pressure and $\mathrm{T}_{ref} = 293$ K is the reference atmospheric temperature.

$$\frac{p_{ref}}{p_a}\frac{1}{2\pi\tau_1} = 24 + 4.04 \times 10^4 h\frac{0.02 + h}{0.391 + h} \tag{3}$$

$$\frac{p_{ref}}{p_a}\frac{1}{2\pi\tau_2} = \Big(\frac{T_{ref}}{T}\Big)^{\frac{1}{2}}(9 + 280he^{-G}) \tag{4}$$

$$G = 4.17\Big[\big(\frac{T_{ref}}{T}\big)^{\frac{1}{3}} - 1\Big] \tag{5}$$

$$h = RH\frac{(p_{sat}/p_{ref})}{p_a/p_{ref}} \tag{6}$$

$$\begin{aligned}\log_{10}(p_{sat}/p_{ref}) &= 10.795[1 - (T_t/T)] - 5.028\log_{10}(T/T_t)\\ &+ 1.504 \times 10^{-4}1 - 10^{-8.29692}[(T/T_t) - 1]\\ &+ 0.42873 \times 10^{-3}10^{-4.76955}[1 - (T_t/T)] - 1 - 2.2195\end{aligned} \tag{7}$$

Conceptual analyses neglect the fourth and fifth terms in Equation 1. In this study, all the terms are considered in the prediction of sonic boom ground signatures. Using small disturbance theory, linear acoustics equations can be augmented to account for thermo-viscous and relaxation effects. Using thermodynamic identities and assuming that the entropy change during propagation is negligible, dispersion relation can be modified as given in Equation 8. In the low frequency range, Equation 8 is reduced to the traditional linear dispersion relation $\kappa = \omega/\mathrm{c}$. The additional terms account for the changes in the dispersion relation due to dissipation and relaxation.

$$k = \frac{\omega}{c} + i\frac{\omega^2}{c^3}\delta + \frac{\gamma - 1}{2c_p}\frac{\omega}{c}\Sigma_\nu\frac{c_{v\nu}}{1 - i\omega\tau_\nu} \tag{8}$$

where

$$\delta = \frac{\mu}{2\rho_0}\left[\frac{4}{3} + \frac{\mu_B}{\mu} + \frac{(\gamma-1)\kappa}{c_p\mu}\right] \tag{9}$$

The above dispersion relation can be re-expressed as given in Equation 10, where Δk_R is the dispersive real wave number and Δk_I is the dispersive imaginary wave number. Expressions for these are given in Equations 11 and 12 respectively.

$$k = \frac{\omega}{c_0} + \Delta k_R + i\Delta k_I \tag{10}$$

$$\Delta k_R = -\frac{\omega}{c^2}\Sigma_\nu(\Delta c)_\nu \frac{(\omega\tau_\nu)^2}{1+(\omega\tau_\nu)^2} \tag{11}$$

$$\Delta k_I = \frac{\omega^2}{c^3}\delta + \frac{\omega}{c^2}\Sigma_\nu(\Delta c)_\nu \frac{\omega\tau_\nu}{1+(\omega\tau_\nu)^2} \tag{12}$$

B. Absorption algorithm

The frequency spectrum analysis of sonic booms has been extensively studied by many researchers [28, 29]. Frequency analysis is useful in determining the loudness of boom signatures as well as response of structures and buildings. After each time domain step, FFT is used to convert the signature to frequency domain. The signature is attenuated by $exp[-k_I\Delta x]$ and shifted in phase using $exp[ik_R\Delta x]$. Figure 9 depicts an algorithmic flowchart used in this study. During the pressure propagation phase, the pressure-time signature is calculated at several altitudes along the ray tube. At each altitude, the pressure signature after non-linear correction is converted into frequency domain, the signature is attenuated according to prevailing meteorological conditions and the new frequency spectrum is converted back into the time domain. This new pressure-time signature is used to replace the prevailing pressure signature at that altitude and this new waveform is used as the starting signature for the next propagation slab till the next altitude. This procedure is continued to the ground level.

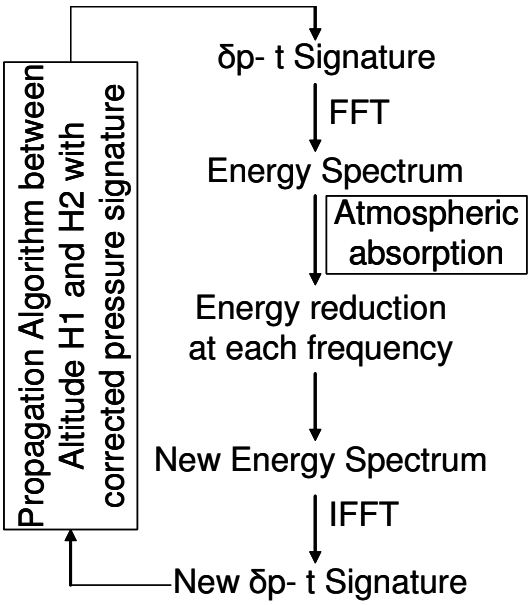

Figure 9. Atmospheric Absorption Algorithm

Figure 10 compares the sonic boom ground signatures obtained using the absorption procedure when propagated from an altitude of 50000 feet and with an assumed gross weight of 80000 lbs for the configuration (See Figure 5) with and without tail. The absorption algorithm requires the specification of atmospheric relative humidity profiles. Figure 10(a) represents such a distribution generated based on observations or predictions of the atmospheric profiles [22,30,31] at various locations and seasons. During the implementation of the absorption algorithm, the FFT and IFFT operations are performed once in every 15 time steps to reduce computational time. This is a good approximation in the propagation of weak shock systems such as sonic booms. Figure 10(b) compares the ground sonic boom signatures. Referring back to Figure 8, the difference is mainly in the rear of the signature where additional shock structure is present in the near field due to the tail geometry. The signature perturbation in the near field has an expansion followed by a compression/shock. As the signature propagates through the atmosphere, the compression waves travel faster than the expansion waves and are reduced in strength as they meet the expansion waves. The additional shocks due to the tail are not strong enough to make their way to the front and coalescence with the front shock system does not occur. Therefore, the front shock system in the ground signature is same for both configurations. However, because of rear shock coalescing, the rear shock strength is increased in magnitude. Furthermore, due to the increased effective length of the near-field signature, the T-tail configuration produces a ground signature which is longer in duration.

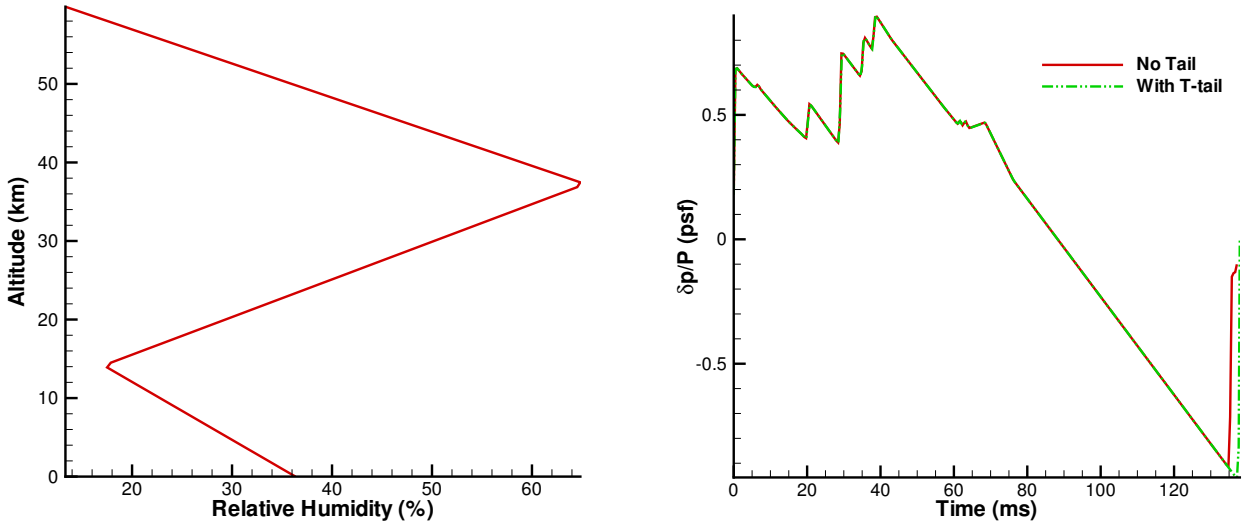

(a) **Relative humidity distribution**

(b) **Ground signature comparison**

Figure 10. Sonic boom ground signature comparison with and without T-tail

V. Application of the new methods to an optimized configuration

This section evaluates one of the optimized configurations obtained using a previous conceptual study [32] using the improved methods described in this paper. The results obtained using traditional methods are compared with those obtained with the improved tools for accuracy and computational time.

In a previous conceptual configuration optimization study [32], various important responses of the system were simultaneously optimized. These include cruise lift to drag ratio, sonic boom loudness level, range, center of gravity excursions, fuel weight etc. Inclusion of many objectives allows conceptual design optimization in various dimensions, which is extremely crucial in the design of complex and revolutionary systems. To obtain globally optimum population of aircraft designs, an advanced hierarchical structured genetic algorithm was used. The genetic algorithm employed an improved crossover operator to allow for better information exchange between reproducing parents, various optimization weighing schemes as well as a parallel feature to result in fast computational turn around time. Figure 11 shows one of the optimized configurations obtained from the optimization study, in different mesh representations automatically generated from the

parametric aircraft configuration. This geometry is evaluated using improved linear methods and automated panel analyses to study the drawbacks and inadequacies of the traditional conceptual methods. As has been explained earlier, panel abutment is achieved using an automated procedure and panel analysis is run. The abutted structured panel configuration is depicted in Figure 11(c). This easy and automated transformation from one representation to another may be perceived as a valuable contribution for conceptual analysis and design.

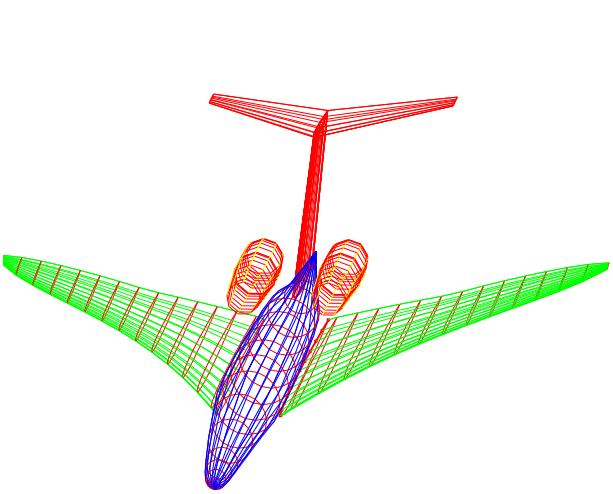

(a) **Geometry representation in traditional methods**

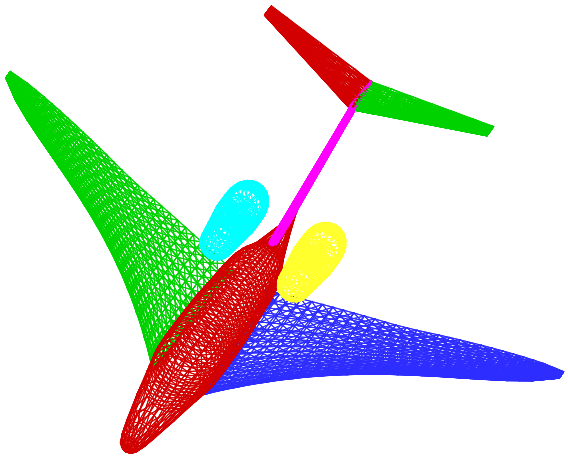

(b) **Unstructured watertight representation**

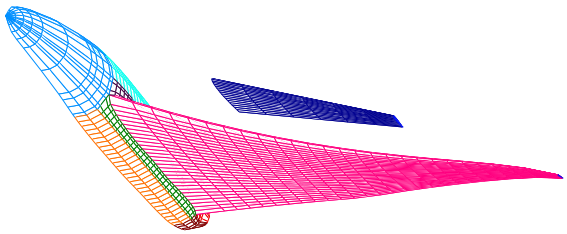

(c) **Structured watertight representation**

Figure 11. Automated geometry representation of an optimized configuration

Figure 12 depicts the PANAIR solution in terms of the surface pressure coefficient over this geometry at a Mach number=1.6 and a trim angle of attack=3.12^o. Some of the results obtained using traditional methods are compared with those obtained using the new conceptual methods in Table 1 for this optimized configuration. Because of accurate computation of equivalent and wetted areas and use of panel analysis as against comparitively low fidelity vortex lattice method [19], results are expected to be more accurate using the new approach. The one striking difference is that the perceived loudness value predicted using the new approach is significantly different. These sort of differences may render the so called optimized configurations into regular non-optimum configurations using high fidelity analysis.

Figure 13 depicts the comparison of the near-field pressure signatures. Traditional methods [10, 11] fail

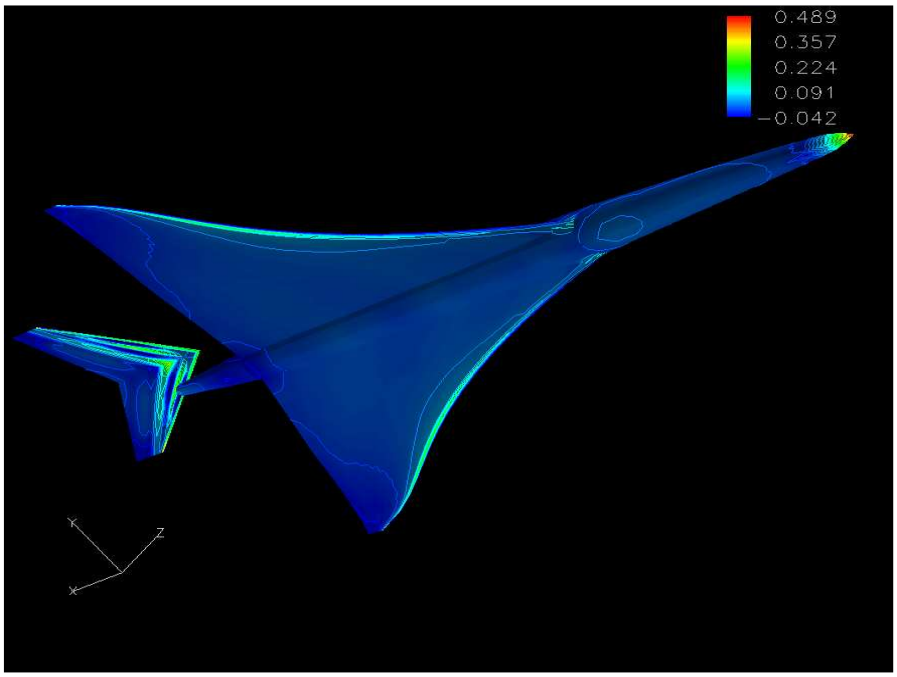

Figure 12. Surface flow solution over an optimized geometry

to capture the three dimensional effects as well as tail effects. It is seen that the shock magnitudes are larger and the shock locations are shifted when PANAIR is used. Figure 14 shows the comparison of the sonic boom ground signatures. Increased shock magnitudes and non-linear shock coalescence effects produce a significant change in the shock overpressure when compared to the traditional methods.Using PANAIR, the ground signature has a considerable shock in the mid portion which is probably due to the merging of tail front shock and wing rear shock. This mid shock is not captured using the traditional method because of the combined effect of the location of wing shock and the tail effects not being modeled properly. The signature duration is very different using the two methods. The time required to run the new conceptual analysis is about 120 seconds compared to about 5 seconds for the existing approach. However, this computational time includes automatic geometry generation, discretization, panel automation and flow solution. This is acceptable, even in conceptual design, given the advantages not only in the fidelity of the results, but also in the flexibility that it offers to run CFD over the conceptual configurations.

Table 1. Comparison of results over the optimized design

Analysis	C_L	C_{Di}	C_{Dw}	C_{Df}	PL (dB)
Linear methods	0.13103	0.0113	0.002	0.0059	88.45
New approach	0.1181	0.0063	0.0044	0.0034	96.43

VI. Conclusions and future work

A set of new automated conceptual methods have been developed for supersonic aircraft design. The geometry generation and discretization procedure enables an efficient and automatic way to combine linearized and non-linear analysis. Automated panel analysis allows for improved fidelity computational results with minimal effort. Atmospheric propagation analysis provides a strategy to include advanced atmospheric

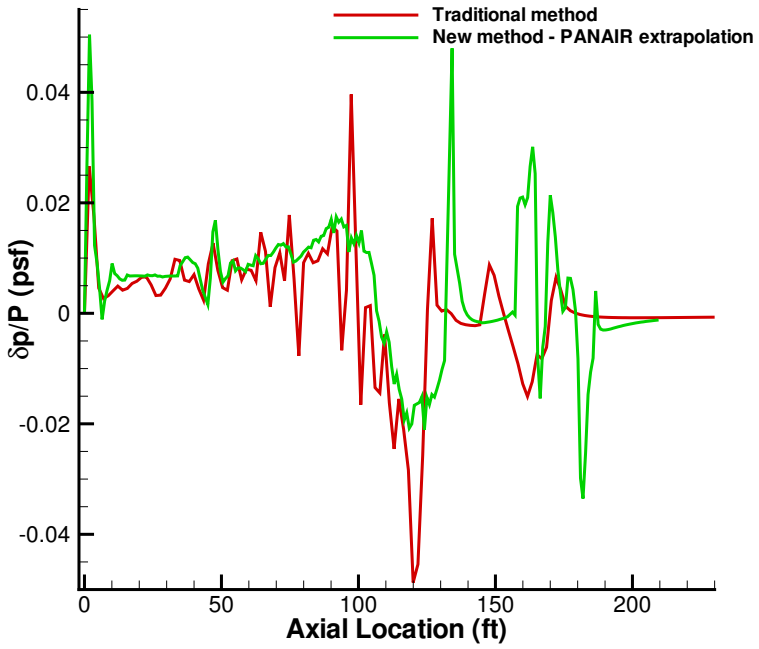

Figure 13. Sonic boom near-field signature comparison

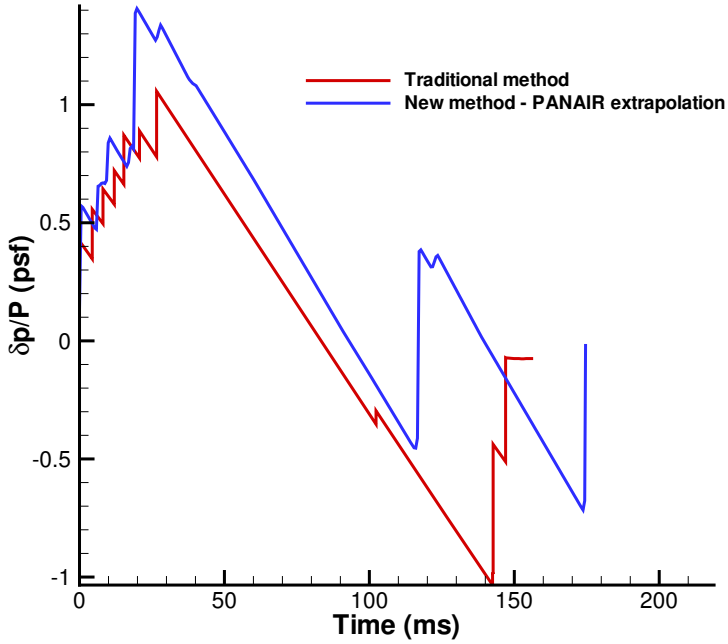

Figure 14. Sonic boom ground signature comparison

effects into the aircraft design process. Using features such as atmospheric absorption and improved near field signature, the present method is expected to produce improved results when compared to the existing methods while not significantly degrading computational time savings. The combination of geometry-based and physics-based analyses in the new method increases the confidence of the results obtained in conceptual design and paves the way for easy integration into a high fidelity architecture. Due to lack of time, optimization using the new methods was not carried out. This will be carried out in future studies.

VII. Acknowledgements

This work was supported under contract NAS1-02117, "Decision Making Support for NASAs Aeronautics Research Mission Directorate", from NASA Langley Research Center with Mr.Craig Nickol as the technical monitor. The authors wish to acknowledge the help offered by Takemiya Tetsushi of the Aerospace Systems Design Lab at Georgia Tech in validating PANAIR results.

References

[1]Darden, C. M., "The importance of sonic boom research in the development of future high speed aircraft," *Journal of the NTA*, Vol. 65, No. 3, 1992, pp. 54–62.

[2]Henne, P. A., "Case for Small Supersonic Civil Aircraft," *Journal of Aircraft*, Vol. 42, No. 3, May 2005, pp. 765–774.

[3]Mavris, D. N. and Delaurentis, D., "Methodology for examining the simultaneous impact of requirements, vehicle characteristics, and technologies on military aircraft design," *22nd Congress of the International Council on the Aeronautical Sciences*, ICAS, Harrogate, England, Aug. 2000.

[4]Buonanno, M. A. and Mavris, D. N., "A New Method for Aircraft Concept Selection Using Multicriteria Interactive Genetic Algorithms," AIAA Paper 2005-1020, Jan. 2005.

[5]Aronstein, D. C. and Schueler, K. L., "Two Supersonic Business Aircraft Conceptual Designs, With and Without Sonic Boom Constraint," *Journal of aircraft*, Vol. 42, No. 3, 2005, pp. 775–786.

[6]Rallabhandi, S. K. and Mavris, D. N., "Aircraft Geometry Design and Optimization for Sonic Boom Reduction," *Journal of Aircraft, Accepted, In Press*, 2006.

[7]Popinet, S., "GNU triangulation surface library," 2005.

[8]Plotkin, K. K. and Page, J. A., "Extrapolation of Sonic Boom Signatures from CFD Solutions," AIAA Paper 2002-922, Jan. 2002.

[9]Rallabhandi, S. K. and Mavris, D. N., "A New Approach for Incorporating Computational Fluid Dynamics into Sonic Boom Prediction," AIAA Paper 2006-3312, June 2006.

[10]Harris, R. V., "An analysis and correlation of Aircraft wave drag," Tech. Rep. NASA TM X-947, NASA, Princeton,NJ, April 1964.

[11]Coen, P. G., "Development of a computer technique for the prediction of transport aircraft flight profile sonic boom signatures," Master's thesis, The George Washington University, March 1991.

[12]Rallabhandi, S. K. and Mavris, D. N., "Sonic Boom Minimization using Improved Linearized Tools and Probabilistic Propagation," AIAA Paper 2005-1019, Jan. 2005.

[13]Rallabhandi, S. K. and Mavris, D. N., "An unstructured wave drag code for preliminary design of future supersonic aircraft," AIAA Paper 2003-3877, June 2003.

[14]Alonso, J. J. and Kroo, I. M., "Advanced algorithms for design and optimization of quiet supersonic platforms," AIAA Paper 2002-144, Jan. 2002.

[15]Choi, S., Alonso, J. J., Kim, S., and Kroo, I. M., "Two-level Multi-Fidelity Design Optimization Studies for Supersonic Jets," AIAA Paper 2005-531, Jan. 2005.

[16]Carmichael, R. L., "Public Domain Aeronautical Software," 2003.

[17]Saaris, G. A., "A502 User's Guide – PAN AIR Technology Program for Solving Problems of Potential Flow about Arbitrary Configurations," Boeing Document D6-53818, June 1998.

[18]Shewchuk, J. R., "Triangle: Engineering a 2D Quality Mesh Generator and Delaunay Triangulator," Philadelphia, PA, May 1996, pp. 124–133.

[19]Miranda, E. and Baker, "A Generalized Vortex Lattice Method for Subsonic and Supersonic Flow Applications," NASA CR-2865, Nov. 1977.

[20]Loving, D. L. and Estabrooks, B. B., "Transonic Wing Investigation in the Langley Eight Foot High Speed Tunnel at High Subsonic Mach Numbers and at a Mach number of 1.2," NACA RM L51F07, Sept. 1951.

[21]Hopkins, E. J., Hicks, R. M., and Carmichael, R. L., "Aerodynamic characteristics of several cranked leading-edge wing-body combinations at Mach numbers from 0.4 to 2.94," NASA TN-D-4211, Oct. 1967.

[22]Blumrich, R., Coulouvrat, F., and Heimann, D., "Meteorologically induced variability of sonic-boom characteristics of supersonic aircraft in cruising flight," *Journal of the Acoustical Society of America*, Vol. 118, No. 2, 2005, pp. 707–722.

[23]Bass, H. E., Raspet, R., Chambers, J. P., and Kelly, M., "Modification of sonic boom wave forms during propagation from the source to the ground," *Journal of Acoustical Society of America*, Vol. 111, No. 1, Jan. 2002, pp. 481–486.

[24]Pierce, A. D. and Maglieri, D. J., "Effects of atmospheric irregularities on sonic boom propagation," *Journal of Acoustical Society of America*, Vol. 51, No. 2, 1972, pp. 702–721.

[25]Plotkin, K. J., "PCBoom3 Sonic boom prediction model - Version 1.0c," Tech. Rep. AFRL-HE-WP-TR-2001-0155, Wyle Research laboratories, Arlington,VA, May 1996.

[26]Cleveland, R. O., Chambers, J. P., Bass, H. E., et al., "Comparison of computer codes for the propagation of sonic boom waveforms through isothermal atmospheres," *Journal of Acoustical Society of America*, Vol. 100, No. 5, Nov. 1996, pp. 3017–3027.

[27]Kang, J., "Nonlinear Acoustic Propagation of Shock Waves Through the Atmosphere with Molecular Relaxation," Ph.D. thesis, Pennsylvania State University, University Park, PA, May 1991.

[28]Brown, J. G. and Haglund, G. T., "Sonic boom loudness study and airplane configuration development," AIAA Paper 1988-4467, Sept. 1990.

[29]Ahuja, K. K., Stevens, J. C., and Walterick, R. E., "A Giant Simulator of Sonic Boom and Aircraft Noise," AIAA Paper 1993-4430, Oct. 1993.

[30]Avila, R., Vernin, J., and Sanchez, L. J., "Atmospheric Turbulence and Wind Profiles Monitoring with Generalized Scidar," *Astronomy and Astrophysics*, Vol. 369, No. 1, April 2001, pp. 364–372.

[31]Sutherland, L. C. and Bass, H. E., "Atmospheric absorption in the atmosphere up to 160 km," *Journal of the Acoustical Society of America*, Vol. 115, No. 3, 2004, pp. 1012–1032.

[32]Buonanno, M. A., "A Method for Aircraft Concept Exploration Using Multicriteria Interactive Genetic Algorithms," Ph.D. thesis, Georgia Institute of Technology, School of Aerospace Engineering, Dec. 2005.